Journal of Alloys and Compounds 509 (2011) 731–734

Contents lists available at ScienceDirect

Journal of Alloys and Compounds

journal homepage: www.elsevier.com/locate/jallcom

The Mn-doping effect on the charge ordering state of $La_{1/3}Sr_{2/3}FeO_3$

Kong Hui [a,*], Kong Zhang-Qing [a], Zhu Changfei [b,**]

[a] School of Metallurgy and Resources, Anhui University of Technology, Maanshan, Anhui 243002, PR China
[b] Laboratory of Advanced Functional Materials and Devices, Department of Materials Science and Engineering, University of Science and Technology of China, Hefei, Anhui 230026, PR China

ARTICLE INFO

Article history:
Received 25 October 2009
Received in revised form 6 September 2010
Accepted 8 September 2010
Available online 17 September 2010

PACS:
62.80.+f
71.38.−k
75.30.Kz

Keywords:
Rare earth compounds and compounds
Oxide materials
Electron–phonon interaction
Ultrasonic

ABSTRACT

The longitudinal ultrasonic velocity (V_l), as well as resistivity has been measured in single-phase polycrystalline $La_{1/3}Sr_{2/3}Fe_{1-x}Mn_xO_3$ ($x = 0$, 0.025, 0.05) at a frequency of 10 MHz, from 20 K to 300 K. It is found that with increasing Mn-doping level, the resistivity increases and the charge ordering transition temperature T_{CO} shifts to lower temperature. For all samples, upon cooling down from 300 K, a substantial softening in V_l above T_{CO} and dramatic stiffening below T_{CO} are observed. This abnormal elastic softening above T_{CO} can be described well by the mean-field theory, which indicates that this feature is due to the electron–phonon coupling via the Jahn–Teller effect and this coupling is enhanced with the Mn doping. Below T_{CO}, another softening in V_l is observed for $x = 0$, and weakens with the increasing of Mn content. This character is attributed to the breathing-type distortion of Fe–O octahedron and suggests that the charge disproportionation (CD) transition is suppressed by the Mn substitution.

1. Introduction

The perovskite-type transition-metal oxides have attracted much attention due to their particular structural, electronic and magnetic properties. Besides the well-known colossal magnetoresistance effect (CMR) [1], another interesting phenomenon is the real-space ordering of charge carriers [2]. Among the charge ordering (CO) systems, $La_{1/3}Sr_{2/3}FeO_3$ has attracted considerable attention because its CO accompanies both antiferromagnetic (AFM) spin ordering and charge disproportionation (CD) of $2Fe^{4+} \rightarrow Fe^{3+} + Fe^{5+}$ [3,4]. And in its ordering state, a sequence of $\ldots Fe^{3+}\ Fe^{3+}\ Fe^{5+}\ Fe^{3+}\ Fe^{3+}\ Fe^{5+}\ldots$ exists along the [1 1 1] direction of the pseudocubic perovskite unit cell [5].

The most novel feature in $La_{1/3}Sr_{2/3}FeO_3$ is the high valence state of Fe:Fe^{4+} and Fe^{5+}. For $Fe^{4+}(d^4)$, it is isoelectronic with Mn^{3+}. From previous works, it has been widely recognized that the Jahn–Teller distortion of Mn^{3+}, plays an important role for the CO state in manganites [6]. Thus the similar lattice distortion is expected in $La_{1/3}Sr_{2/3}FeO_3$. And for Fe^{5+}, it occupies smaller octahedral sites than Fe^{3+}, which would results in the breathing-type distortion of Fe–O octahedron. In fact, the difference of the Fe–O bond lengths was found in the charge disproportionation transition of $CaFeO_3$, which is higher than 0.1 Å [7]. However, the existence of these two kinds of lattice distortion in $La_{1/3}Sr_{2/3}FeO_3$ is still under discussion. Different conclusions have been drawn through different experimental and theoretical tools, which are summarized as follows.

First, no structural changes accompany the CO–CD transition. This point was supported by the neutron powder diffraction results [5]. And unrestricted Hartree–Fock band-structure calculations have also suggested that this charge ordering can be driven by purely electronic interactions [8]. Second, only the breathing-type distortion of Fe–O octahedron exists below T_{CO}. This explanation was based on the fact of the superlattice spots, which have been detected by the transmission electron microscopy below T_{CO} [3]. Ishikawa also confirmed this distortion by the measurement of optical spectroscopy [9]. Third, the lattice distortions are present only above T_{CO}. In 2005, Ghosh et al. indicates this result from the temperature-dependent micro-Raman study [10].

From these works, it can be seen that the physical nature for this threefold CO–CD phase is still controversial. And the attention of researchers was mainly concentrated on the question: whether this transition is accompanied by any lattice distortions? Thus, a detailed revelation of the interplay between the lattice dynamics and the CO–CD transition in $La_{1/3}Sr_{2/3}FeO_3$ remains to be resolved and more experimental tools and results are needed.

The ultrasonic technique is a sensitive tool for studying the lattice distortion and has been successfully employed to study the CO

* Corresponding author. Tel.: +86 0555 2315180.
** Corresponding author. Tel.: +86 0551 3602938.
E-mail addresses: konghui@ahut.edu.cn (H. Kong), cfzhu@ustc.edu.cn (C. Zhu).

0925-8388/$ – see front matter © 2010 Elsevier B.V. All rights reserved.
doi:10.1016/j.jallcom.2010.09.038

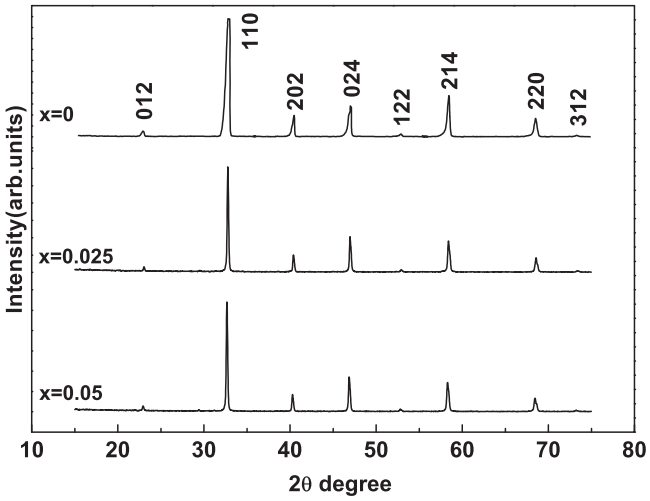

Fig. 1. XRD patterns of $La_{1/3}Sr_{2/3}Fe_{1-x}Mn_xO_3$ ($x = 0$, 0.025, 0.05) at room temperature.

state in manganites [6] and the CO–CD transition in $La_{1/3}Sr_{2/3}FeO_3$ [11,12]. This technique provided new evidence to support the two kinds of lattice distortion in the CO–CD process. However, this conclusion needs more experimental supports. Since the high-valence state of Fe^{5+} in $La_{1/3}Sr_{2/3}FeO_3$ is stabilized by the strong hybridization with O 2*p* bands [9], its stability is very sensitive to the surrounding environment. So the B-site doping effect is believed to provide important clues to the nature of the CO–CD transition [12]. In this paper, we report our systematic studies of the longitudinal ultrasonic velocity (V_l) as a function of temperature in $La_{1/3}Sr_{2/3}Fe_{1-x}Mn_xO_3$ ($x = 0$, 0.025, 0.05) with an aim to gain more insight into the microscopic origin of CO–CD transition.

2. Experimental procedure

The polycrystalline samples of $La_{1/3}Sr_{2/3}Fe_{1-x}Mn_xO_3$ ($x = 0$, 0.025, 0.05) were prepared by a solid-state reaction method. Stoichiometric amount of high purity La_2O_3, $SrCO_3$, $MnCO_3$ and Fe_2O_3 powders were well mixed, ground and calcinated at 1100°, 1150°, 1200° in air for 15 h. The final obtained powder was then pressed into pellets at 300 MPa and sintered at 1200° in air for 20 h.

The crystal structure was characterized using a Japan Rigaku MAX-RD powder X-ray diffractometer with Cu Kα radiation (λ = 1.5418 Å) at room temperature. The resistivity was measured by the standard four-probe technique. The longitudinal ultrasonic velocity measurement was performed on the Matec-7700 series by means of a conventional pulsed echo technique. All experiments were taken in a closed-cycle refrigerator during the warm-up from 20 to 300 K at the rate of about 0.25 K/min. Temperature was measured with an Rh–Fe resistance thermometer. The estimated error on temperature is ±0.1 K.

The relative change of the longitudinal sound velocity $\Delta V_l/V_{l\min}$ in Fig. 3 was defined according to the following equation:

$$\frac{\Delta V_l}{V_{l\min}} = \frac{V_l - V_{l\min}}{V_{l\min}} \quad (1)$$

where $V_{l\min}$ ($m\,s^{-1}$) is the minimal longitudinal sound velocity in the temperature range from 20 K to 300 K.

3. Experimental results and discussion

The X-ray diffraction patterns of $La_{1/3}Sr_{2/3}Fe_{1-x}Mn_xO_3$ ($x = 0$, 0.025, 0.05) are shown in Fig. 1. All samples are of single phase with no detectable secondary phases. The diffraction peaks are sharp and can be indexed with the space group $R\bar{3}c$ in the hexagonal setting, which are consistent with other reports [4].

Fig. 2(a) exhibits the temperature dependence of resistivity for $La_{1/3}Sr_{2/3}Fe_{1-x}Mn_xO_3$ ($x = 0$, 0.025, 0.05). All samples show semiconductor-like transport behavior in the whole temperature range, which increases slightly with Mn doping, and exhibit a discernible slope change around the T_{CO}. To study the evolution of CO transition in $La_{1/3}Sr_{2/3}Fe_{1-x}Mn_xO_3$, the $d(\ln\rho)/d(T^{-1}) - T$ curves

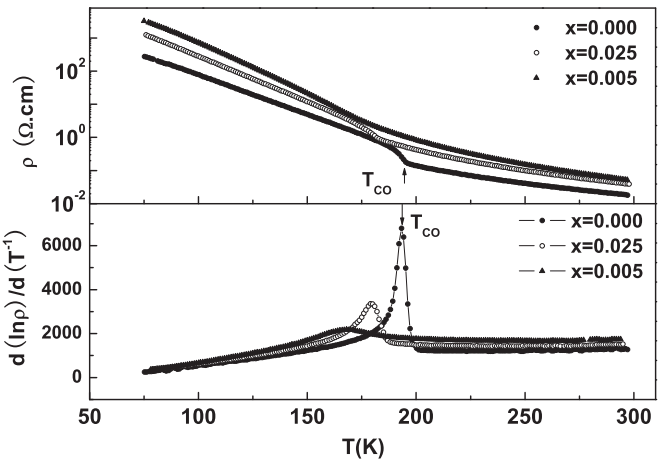

Fig. 2. Variations of (a) the resistivity ρ and (b) the logarithmic derivative, $d(\ln\rho)/d(T^{-1})$, of the resistivity with temperature for $La_{1/3}Sr_{2/3}Fe_{1-x}Mn_xO_3$ ($x = 0$, 0.025, 0.05).

were plotted in the Fig. 2(b). All curves show an abnormal peak, and according to the previous studies, the T_{CO} can be defined as the corresponding peak temperature [13]. It can be seen that with increasing Mn doping level, the CO state becomes unstable: the T_{CO} shifts to lower temperature, and the peak of $d(\ln\rho)/d(T^{-1})$ is broadened. Furthermore, the peak value of $d(\ln\rho)/d(T^{-1})$ decreases from more than 6000 in the Mn-free sample to about 2000 in $x = 0.05$ sample. This behavior is due to the substitution of Mn^{3+} for Fe^{3+}. The doped Mn acts as an impurity, inducing disorder and hindering the establishing of antiferromagnetic charge ordering state. The similar disorder effect has been well discussed in charge-ordered manganites [14].

Fig. 3 shows the temperature dependence of the longitudinal ultrasonic velocity (V_l) at a frequency of 10 MHz for $La_{1/3}Sr_{2/3}Fe_{1-x}Mn_xO_3$ ($x = 0$, 0.025, 0.05). In all samples, the V_l softens smoothly as the temperature decreasing from 300 K and substantially increases below T_{CO}, which exhibits a valley around T_{CO}. Below 181 K, the V_l of $La_{1/3}Sr_{2/3}FeO_3$ shows another unexpected softening and resumes normal increase at about 70 K. With Mn doping, this anomaly weakens and finally disappears for $x = 0.05$. It is well known that in the normal state, the ultrasonic

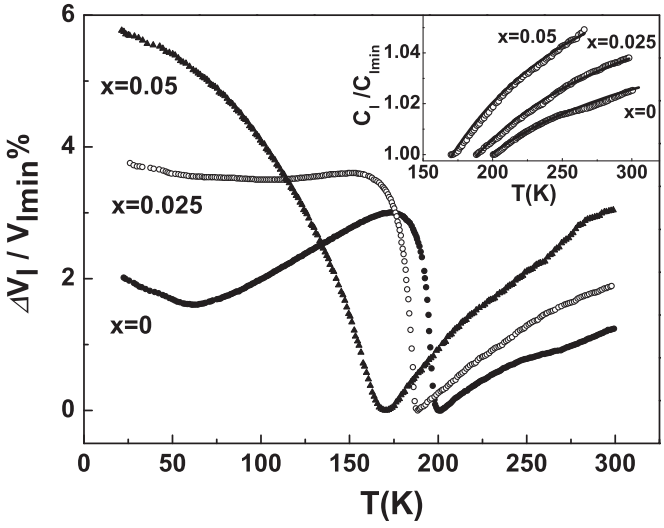

Fig. 3. The temperature dependence of the longitudinal ultrasonic velocity for $La_{1/3}Sr_{2/3}Fe_{1-x}Mn_xO_3$ ($x = 0$, 0.025, 0.05). The inset is the temperature dependence of the $C_l(T)$ for $La_{1/3}Sr_{2/3}Fe_{1-x}Mn_xO_3$ ($x = 0$, 0.025, 0.05) above T_{CO} (open symbols are experimental data, solid line is the results calculated using Eq. (2)).

velocity increases with the temperature decreasing. Thus the origin of these two kinds of velocity softening needs explanations.

As is known, the charge-ordering transition in $La_{1/3}Sr_{2/3}FeO_3$ is accompanied by the AFM transition. Thus, the first consideration of the origin of the ultrasonic anomaly around T_{CO} is the magnetic transition. According to the Landau–Khalatnilov theory, the relative velocity change ($\Delta V/V$) caused by a typical AFM spin fluctuations is of the order 0.1% [15]. However, in $La_{1/3}Sr_{2/3}Fe_{1-x}Mn_xO_3$, the $\Delta V/V$ around T_{CO} is more than 3%, which is much larger than that caused by an AFM phase transition. These results indicate that there is a strong electron–phonon coupling in this system. In fact, the similar phenomenon has been well discussed in charge-ordered manganites on both experimental and theoretical levels [6,16], which is interpreted by the electron–phonon coupling originated from the Jahn–Teller effect of Mn^{3+}. Thus it is reasonable to attribute this ultrasonic anomaly in $La_{1/3}Sr_{2/3}Fe_{1-x}Mn_xO_3$ to the similar electron–phonon coupling. However, the question is: which kind of transition-metal ions is Jahn–Teller active?

In $La_{1/3}Sr_{2/3}Fe_{1-x}Mn_xO_3$, Mn^{3+} is the first candidate for the Jahn–Teller effect. However, in $x = 0$ sample, no Mn^{3+} exist, which suggests that the Mn^{3+} could not response to the ultrasonic anomalies in $La_{1/3}Sr_{2/3}Fe_{1-x}Mn_xO_3$ alone. Thus the Fe ions should be considered. For Fe ions, the experimental results showed that its valence states are +3 and +4 above T_{CO} [4]. The ground state of Fe^{3+} is high-spin $t_{2g}{}^3e_g{}^2$ with two unpaired electrons filling the e_g band, which means Fe^{3+} does not necessarily remove the degeneracy to low its symmetry. So it is not Jahn–Teller active. For Fe^{4+}, due to its unconventionally high valence, the electronic structure is rather unique. It is isoelectronic with Mn^{3+} and its charge-transfer energy Δ is quite negative, which implies that a large amount of charges are transferred via Fe–O bonds from the O 2*p* bands to the Fe *d* orbits. Thus the Fe^{4+} state is a mixture of $3d^4$ and $3d^5\underline{L}$ [17], where $\underline{L}$ denotes a hole in the O 2*p* band, and the $3d^4$ state may be Jahn–Teller active.

To clarify the relationship between the ultrasonic anomaly and Jahn–Teller effect, the ultrasonic velocity data were analyzed by the Jahn–Teller theory, which describes the coupling of the Jahn–Teller ions to the lattice distortion under the mean field approximation. According to this theory, the relationship between the longitudinal modulus $C_l(T)$ and temperature $T(T > T_{CO})$ can be written as [18]:

$$C_l(T) = C_0\left(\frac{T - T_C^0}{T - \Theta}\right) \quad (2)$$

where $C_l = DV_l^2$ [19], with D is the mass density, C_0 is the elastic modulus in the absence of Jahn–Teller coupling of the lattice with the electronics state of the ions, and the characteristic temperature of T_C^0 and Θ can be determined by the ultrasonic measurements of the elastic modulus softening. The Jahn–Teller coupling energy E_{JT} is obtained by the formula [$E_{JT} = T_C^0 - \Theta$].

Eq. (2) can be used to fit the experimental data of the elastic softening above T_{CO}, and is proven in charge-ordered manganites [20] and $R_{1/3}Sr_{2/3}FeO_3$ (R = La, Pr, Gd) [21]. The temperature dependence of C_l for $La_{1/3}Sr_{2/3}Fe_{1-x}Mn_xO_3$ ($x = 0$, 0.025, 0.05) is plotted in the inset of Fig. 3. The open symbols are the experimental data and the solid line is the theoretical result (the values of the T_C^0, Θ, C_0/C_{min} are 49.55 K, 39.69 K, 1.066 for $x = 0$ sample, 51.29 K, 38.88 K, 1.090 for $x = 0.025$ sample, and 53.15 K, 39.69 K, 1.114 for $x = 0.05$ sample). The good agreement between experiment and theory indicates that the electron–phonon coupling via the Jahn–Teller effect indeed exists in $La_{1/3}Sr_{2/3}Fe_{1-x}Mn_xO_3$ samples. And from this theoretical calculation results, it can be seen that the E_{JT} of $x = 0$, $x = 0.025$ and $x = 0.05$ samples are 9.86 K, 12.41 K and 13.46 K respectively. The increase of E_{JT} as Mn content increasing reflects that the coupling of Jahn–Teller effect becomes stronger.

Below T_{CO}, another equation can be used to describes the relationship between the $C_l(T)$ and temperature $T(T < T_{CO})$ [18], which is already applied to the charge-ordered manganites [14]. However, in $La_{1/3}Sr_{2/3}Fe_{1-x}Mn_xO_3$ system, the CD transition occurs below T_{CO}, and the interplay among different valence states of iron (Fe^{3+}, Fe^{4+}, Fe^{5+}) makes this quantitative equation invalid. Thus, to prove that the hardening of V_l below T_{CO} also originates from the Jahn–Teller effect, two theoretical qualitative results are applied to the $La_{1/3}Sr_{2/3}Fe_{1-x}Mn_xO_3$ samples.

First, based on the Hamiltonian of small Jahn–Teller polarons with strong electron–phonon coupling, Min et al. found that in manganites, the CO interaction induces the softening of V_l above T_{CO} and the hardening below T_{CO} [16], which is proven in the charge-ordered manganites [6,14]. Their calculation result is qualitatively similar to our observation.

Second, from earlier studies in manganites, the relative stiffening of the ultrasonic velocity can be viewed as a scale of the development of the Jahn–Teller effect [6]. And this conclusion was proved in the in the low Sr-doping $La_{1-x}Sr_xFeO_3$ [22], which corresponds to the short-range charge ordering state of Fe^{3+} and Fe^{4+}. So if the Jahn–Teller effect indeed exists in the $La_{1/3}Sr_{2/3}Fe_{1-x}Mn_xO_3$ samples during the CO transition, the increase of E_{JT} as Mn content increasing according to the Eq. (2) would lead to more sound velocity increase below T_{CO}. This prediction was proven from the Fig. 3. It can be seen that the relative stiffening of V_l below T_{CO} indeed becomes larger with increasing Mn content. For example, the relative stiffening change of V_l in $x = 0$ sample is only 3%, while it reaches more than 5% in $x = 0.05$ sample.

Based on the upper discussions, it can be seen that the hardening of V_l below T_{CO} in $La_{1/3}Sr_{2/3}Fe_{1-x}Mn_xO_3$ samples is consistent with the qualitative theories, which implies that it may also originate from the Jahn–Teller effect.

It is worth mentioned that both the quantitative calculation of the elastic softening above T_{CO} and qualitative analysis of the velocity hardening below T_{CO} show that with the Mn content increasing, the E_{JT} increases. This behavior is probably due to the following two reasons.

On the one hand, the Mn^{3+} is also Jahn–Teller active. Furthermore, the Jahn–Teller effect of Mn^{3+} is much more than that of Fe^{4+}. For example, in $La_{1/3}Sr_{2/3}MnO_3$, the relative ultrasonic stiffening change is more than 15% [11], and in some charge ordered manganites, the resulting structure change can be detected by the XRD measurement [23]. So its doping would enhance the Jahn–Teller effect.

On the other hand, the doped Mn ion acts as an impurity, making the Fe^{5+} unstable. It is known that the charge disproportionation of $2Fe^{4+} \rightarrow Fe^{3+} + Fe^{5+}$ occurs below T_{CO}, and this transition decreases the content of high-spin Fe^{4+}. For Fe^{5+}, due to its unconventionally high valence, it is stabilized via the strong *p*–*d* hybridization between oxygen 2*p* σ and Fe 3*d* e_g states. From the earlier studies, it is known that the electronegativity of Mn (1.55) is smaller than that of Fe (1.83). So the substitution of Mn increases the electronegativity difference between B-site ion and oxygen, and increases the ionic characteristic of the B–O bond. This feature results in the shift of the intermediate oxygen towards Mn^{3+} and weakens the hybridization between O^{2-} and Fe^{5+}, which makes the Fe^{5+} unstable. Thus the Mn doping would suppress the CD transition and more Fe^{4+} would exist below T_{CO}, which leads to the more velocity stiffening.

If this deduction is true, this suppression would also decrease the fraction of Fe^{5+} below T_{CO} and weaken the breathing-type distortion. To verify this prediction, we focus on the ultrasonic behavior of $La_{1/3}Sr_{2/3}Fe_{1-x}Mn_xO_3$ below T_{CO} in Fig. 3. Below T_{CO}, another unexpected softening in V_l of $La_{1/3}Sr_{2/3}FeO_3$ was observed. From previous reports, it is known that this velocity softening below T_{CO} originates from the breathing type distortion

[11,20]. This distortion arises from the fact that Fe^{5+} cations will occupy smaller octahedral sites than Fe^{3+} cations, and was confirmed by the measurements of transmission electron microscopy [3] and optical spectroscopy [9]. So if the Mn doping indeed suppresses the charge disproportionation in $La_{1/3}Sr_{2/3}FeO_3$, this breathing-type distortion would be weakened. For example, in $La_{1/3}Sr_{2/3}Fe_{1-x}Co_xO_3$, the softening in V_l below T_{CO} weakens with the Co doping [12]. Accompanying this variation, the Mössbauer spectroscopy measurement indicates that the fraction of Fe^{5+} decreases from 33% in $La_{1/3}Sr_{2/3}FeO_3$ at 20 K [4] to 17% in $La_{1/3}Sr_{2/3}Fe_{0.85}Co_{0.15}O_3$ at 15 K [24]. From Fig. 3, it can be seen that the ultrasonic softening below T_{CO} weakens with the Mn doping and finally disappears at $x = 0.05$. This feature is consistent with our analysis and implies that the Mn doping indeed suppress the CD transition. However, the Mössbauer spectroscopy results would be valuable to further clarify the evolution of this transition.

Based on the upper discussions, it can be seen that the Mn doping not only enhances the Jahn–Teller effect, but also suppresses the CD transition. Both these effects lead to more sound velocity increasing below T_{CO}.

4. Conclusion

In conclusion, we have systemically studied the ultrasonic properties of polycrystalline $La_{1/3}Sr_{2/3}Fe_{1-x}Mn_xO_3$ ($x = 0, 0.025, 0.05$) to clarify the Mn doping effect on the CO–CD transitions. It is found that the Mn substitution increases the resistivity and T_{CO} shifts to lower temperature. Dramatic softening in V_l above T_{CO} is observed in all samples, which can be described well by the mean-field theory. Below T_{CO}, another softening in V_l is observed for $x = 0$, and weakens as the Mn content increases. These results indicate that two kinds of lattice distortion exist in $La_{1/3}Sr_{2/3}Fe_{1-x}Mn_xO_3$ samples. The first is the distortion arising from the Jahn–Teller effect of high-spin Fe^{4+}, which is present around T_{CO} and leads to the softening in V_l above T_{CO} and the stiffening below T_{CO}. When the CD transition occurs, the Fe^{4+} gradually changed to Fe^{3+} and Fe^{5+}, and the Jahn–Teller type distortion was replaced by the breathing-type distortion, which results in another softening in V_l at low temperature. With the Mn doping, the E_{JT} increases and the charge disproportionation transition is suppressed. The former increases the velocity stiffening below T_{CO}, and the latter weakens the ultrasonic softening at low temperature. These results are helpful to understand the relationship between the electron–phonon interaction and the CO–CD transitions.

Acknowledgments

This work was supported by the National Natural Science Foundation of China (No. 10774136 and No. 11004002) and the Key Program of Scientific Research Fund of Anhui Provincial Education Department (No. KJ2008A018).

References

[1] R. von Helmolt, J. Wecker, B. Holzapfel, L. Schultz, K. Samwer, Phys. Rev. Lett. 71 (1993) 2331–2333.
[2] C.N.R. Rao, B. Raveau, Colossal Magnetoresistance, Charge Ordering and Related Properties of Manganese Oxides, World Scientific, Singapore, 1998.
[3] J.Q. Li, Y. Matsui, S.K. Park, Y. Tokura, Phys. Rev. Lett. 79 (1997) 297–300.
[4] J.B. Yang, X.D. Zhou, Z. Chu, W.M. Hikal, Q. Cai, J.C. Ho, D.C. Kundaliya, W.B. Yelon, W.J. James, H.U. Anderson, H.H. Hamdeh, S.K. Malik, J. Phys.: Condens. Matter 15 (2003) 5093–5102.
[5] P.D. Battle, T.C. Gibb, P. Lightfoot, J. Solid State Chem. 84 (1990) 271–279.
[6] R.K. Zheng, G. Li, Y. Yang, A.N. Tang, W. Wang, T. Qian, X.G. Li, Phys. Rev. B 70 (2004) 014408–014414.
[7] P.M. Woodward, D.E. Cox, E. Moshopoulou, A.W. Sleight, S. Morimoto, Phys. Rev. B 62 (2000) 844–855.
[8] J. Matsuno, T. Mizokawa, A. Fujimori, K. Mamiya, Y. Takeda, S. Kawasaki, M. Takano, Phys. Rev. B 60 (1999) 4605–4608.
[9] S.K. Park, T. Ishikawa, Y. Tokura, J.Q. Li, Y. Matsui, Phys. Rev. B 60 (1999) 10788–10795.
[10] S. Ghosh, N. Kamaraju, M. Seto, A. Fujimori, Y. Takeda, S. Ishiwata, S. Kawasaki, M. Azuma, M. Takano, A.K. Sood, Phys. Rev. B 71 (2005) 245110–245116.
[11] H. Kong, C. Zhu, Appl. Phys. Lett. 88 (2006) 041920–041922.
[12] H. Kong, Y. Liu, C. Zhu, J. Alloys Compd. 429 (2007) 60–63.
[13] A.P. Ramirez, P. Schiffer, S.-W. Cheong, C.H. Chen, W. Bao, T.T.M. Palstra, P.L. Gammel, D.J. Bishop, B. Zegarski, Phys. Rev. Lett. 76 (1996) 3188–3191.
[14] H.-D. Zhou, G. Li, H. Chen, R.-K. Zheng, X.-J. Fan, X.-G. Li, J. Phys.: Condens. Matter 13 (2001) 6195–6202.
[15] D. Berlincourt, H. Jaffe, Phys. Rev. 111 (1958) 143–148.
[16] B.I. Min, J.D. Lee, S.J. Youn, J. Magn. Magn. Mater. 171 (1998) 881–883.
[17] M. Abbate, F.M.F. de Groot, J.C. Fuggle, A. Fujimori, O. Strebel, F. Lopez, M. Domke, G. Kaindl, G.A. Sawatzky, M. Takano, Y. Takeda, H. Eisaki, S. Uchida, Phys. Rev. B 46 (1992) 4511–4519.
[18] R.L. Melcher, in: W.P. Maston, R.N. Thurston (Eds.), Physical Acoustics, vol. 12, Academic, New York, 1970, pp. 1–21.
[19] M. Cankurtaran, G.A. Saunders, K.C. Goretta, R.B. Poeppel, Phys. Rev. B 46 (1992) 1157–1165.
[20] T. Qian, R.K. Zheng, T. Zhang, T.F. Zhou, W.B. Wu, X.G. Li, Phys. Rev. B 72 (2005) 024432–024438.
[21] H. Kong, C. Zhu, Europhys. Lett. 86 (2009) 54001–54005.
[22] H. Kong, C. Zhu, J. Phys.: Condens. Matter 20 (2008) 115211–115214.
[23] X.-G. Li, H. Chen, C.F. Zhu, H.D. Zhou, R.K. Zheng, J.H. Zhang, L. Chen, Appl. Phys. Lett. 76 (2000) 1173–1175.
[24] P. Adler, S. Ghosh, Solid State Sci. 5 (2003) 445–450.